1. Report No.	2. Government Accession No.	3. Recipient's Catalog No.
FHWA/TX-05/0-1707-5		

4. Title and Subtitle	5. Report Date
SENSITIVITY OF HMA PERFORMANCE TO AGGREGATE SHAPE MEASURED USING CONVENTIONAL AND IMAGE ANALYSIS METHODS	July 2005 Resubmitted: May 2006 Published September 2006
	6. Performing Organization Code

7. Author(s)	8. Performing Organization Report No.
Rajni Sukhwani, Dallas Little, and Eyad Masad	Report 0-1707-5

9. Performing Organization Name and Address	10. Work Unit No. (TRAIS)
Texas Transportation Institute The Texas A&M University System College Station, Texas 77843-3135	11. Contract or Grant No. Project 0-1707

12. Sponsoring Agency Name and Address	13. Type of Report and Period Covered
Texas Department of Transportation Research and Technology Implementation Office P. O. Box 5080 Austin, Texas 78763-5080	Technical Report: February 2000 – September 2003
	14. Sponsoring Agency Code

15. Supplementary Notes

Project performed in cooperation with the Texas Department of Transportation and the Federal Highway Administration

Project Title: Long-Term Research on Bituminous Coarse Aggregate

URL:http://tti.tamu.edu/documents/0-1707-5.pdf

16. Abstract

There is a consensus among researchers and practitioners that aggregate shape properties affect performance, but a debate has arisen over the ability of the current tests to quantify these properties. Recent studies show image analysis techniques to be rapid and provide detailed information on the different shape properties. However, there is a need to compare the results from the image analysis methods with those from conventional tests based on Hot Mix Asphalt (HMA) performance. The focus of this project is on the evaluation of the sensitivity of HMA performance to aggregate properties measured using conventional and image analysis methods. Wavelet image analysis is used to measure texture. Image analysis methods based on the changes in the gradient on a particle boundary, and the difference between a particle radius in a certain direction and that of an equivalent ellipse are used to quantify angularity. Form is quantified by a method that evaluates the changes in particle radii with a fixed incremental change in the central angle. Researchers measured the performance of HMA mixes with different aggregates using the asphalt pavement analyzer (APA), Hamburg wheel tracking device (HW), and dynamic modulus test (DM). In general, the results show that the image analysis methods used in this project had a better correlation with performance than the conventional methods.

17. Key Words	18. Distribution Statement
Image Analysis, Aggregate, HMA, Performance	No restrictions. This document is available to the public through NTIS: National Technical Information Service Springfield, Virginia 22161 http://www.ntis.gov

19. Security Classif.(of this report)	20. Security Classif.(of this page)	21. No. of Pages	22. Price
Unclassified	Unclassified	36	

SENSITIVITY OF HMA PERFORMANCE TO AGGREGATE SHAPE MEASURED USING CONVENTIONAL AND IMAGE ANALYSIS METHODS

by

Rajni Sukhwani
Graduate Research Assistant
Texas A&M University

Dallas Little
Senior Research Fellow
Texas Transportation Institute

and

Eyad Masad
Research Engineer
Texas Transportation Institute

Report 0-1707-5
Project 0-1707
Project Title: Long-Term Research on Bituminous Coarse Aggregate

Performed in cooperation with the
Texas Department of Transportation
and the
Federal Highway Administration

July 2005
Resubmitted: May 2006
Published September 2006

TEXAS TRANSPORTATION INSTITUTE
The Texas A&M University System
College Station, Texas 77843-3135

DISCLAIMER

The contents of this report reflect the views of the authors, who are responsible for the opinions, findings, and conclusions presented herein. The contents do not necessarily reflect the official views or policies of the Texas Department of Transportation (TxDOT) or the Federal Highway Administration (FHWA). This report does not constitute a standard, specification, or regulation. Additionally, this report is not intended for construction, bidding, or permit purposes. Dr. Dallas N. Little, P.E. (#40392) is the principal investigator for the project.

ACKNOWLEDGMENTS

The authors wish to thank Ms. Caroline Herrera of the Construction Division of TxDOT for her guidance and support during this project. We also thank TxDOT and FHWA for their cooperative sponsorship of this project.

TABLE OF CONTENTS

LIST OF FIGURES

LIST OF TABLES

Table **Page**

CHAPTER I
INTRODUCTION

Shape has a great impact on the performance of hot mix asphalt (HMA) [McGennis et al. 1995]. Angular and rough textured aggregates promote interlocking among aggregates in HMA and accordingly, they are desirable physical properties in order to produce mixtures that resist permanent deformation. On the other hand, the presence of flat and elongated aggregate particles is undesirable in HMA. Such particles tend to develop poor resilient properties in the mix, are more susceptible to permanent deformation, and break down during construction. Therefore, these properties need to be carefully measured and monitored in HMA production.

In the current Superpave system, technicians determine coarse aggregate angularity by manually counting the number of fractured faces (ASTM D 5821) (American Society for Testing and Materials). Fine aggregate angularity is measured by the uncompacted void content in a sample of fine aggregate that is poured into a calibrated cylinder after flowing through a standard funnel (Method A, AASHTO T304)(American Association of State Highway and Transportation Officials). Researchers normally use proportional caliper to determine the form (flat and elongation) of coarse aggregate particles (ASTM D 4791).

Fine aggregate angularity tests cannot always discern between poor and good performing aggregates [Huber et al. 1998]. Packing properties (i.e., uncompacted voids) of aggregate are not only a function of angularity, but are also affected by surface texture, gradation, and aggregate specific gravity. Furthermore, the test methods for measuring coarse aggregate properties are laborious, and it is often difficult to test a large enough aggregate quantity to be considered as a representative sample. These tests are also subjective due to the fact that the determination of the degree of flatness and elongation is based on visual inspection. In addition, the current flat-elongation procedure yields a single index reflecting the proportion of aggregates that exceeds a predetermined average dimension ratio. This method is far less descriptive than a probabilistic method for summarizing the results. Another limitation of the current Superpave aggregate shape tests is that two distinct and unrelated tests are required to measure the angularity of coarse and fine aggregates.

Recently, we have witnessed a number of advances in the field of imaging techniques. Electronic and computerized imaging systems offer a great opportunity to speed aggregates characterization. Researchers now view image analysis techniques for determining aggregate properties as a viable and cost-effective alternative. They are fast, dependable, and accurate methods. There is an initial cost involved in setting up a system; however, benefits could easily overshadow the initial costs by recouping the initial investment through extended pavement life [Masad 2003].

The main goal of this project is to evaluate the sensitivity of HMA performance to aggregate properties measured using conventional and image analysis methods. The specific objectives of this project are:

- Quantify angularity, form, and surface texture of both fine and coarse aggregates.

- Correlate aggregate shape properties as classified by image analysis techniques with performance.
- Determine whether surface properties characterized using image analysis techniques are superior to conventional tests in terms of their correlation to performance.

CHAPTER II
MEASUREMENTS OF AGGREGATE PROPERTIES

This section describes the image analysis techniques and conventional methods researchers use to measure the aggregate shape properties. It also presents the materials used in this project.

Image Analysis Methods

A particle shape can be fully expressed in terms of three independent properties: form, angularity, and surface texture [Masad et al. 2001, Masad 2003]. Form reflects variations in the proportions of an aggregate. Angularity reflects variations at the corners; that is, variations superimposed on form. Surface texture is used to describe the surface irregularity at a scale that is too small to affect the overall shape. These three properties can be distinguished because of their different scales with respect to an aggregate size.

Form and angularity are analyzed using black and white images as shown in Figure 1. Particle form is quantified by the summation of the incremental changes in a particle radius in all directions. Radius is defined as the length of the line that connects the particle center to points on the boundary. Eq. (1) gives the form index (FI):

$$\text{Form Index} = \sum_{\theta=0}^{\theta=355} \frac{\left| R_{\theta+5} - R_{\theta} \right|}{R_{\theta}} \qquad (1)$$

where R is the radius of the particle in different directions, and θ is the angle in different directions. The changes in radii are measured with a fixed change in the central angle equal to 5 degrees.

Angularity is analyzed using both the radius and gradient methods. The radius method quantifies angularity by the difference between a particle radius in a certain direction and that of an equivalent ellipse (Figure 2). The equivalent ellipse has the same major and minor axes as the particle, but has no angularity. Normalizing the measurements to the radius of an equivalent ellipse minimizes the effect of form on this angularity index. The angularity index using the radius method is expressed as:

$$\text{Angularity Index-Radius Method} = \sum_{0-0}^{0-355} \frac{R_0 - R_{EE0}}{R_{EE0}} \qquad (2)$$

where R_θ is the radius of the particle at a directional angle θ , and $R_{EE\theta}$ is the radius of an equivalent ellipse at a directional angle θ. Figure 2 shows an illustration of the radii used in Eqs. (1) and (2).

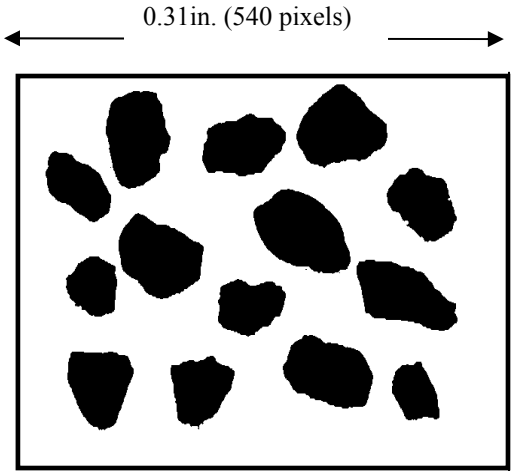

Figure 1. An Example of an Image Used in Form and Angularity Analyses.

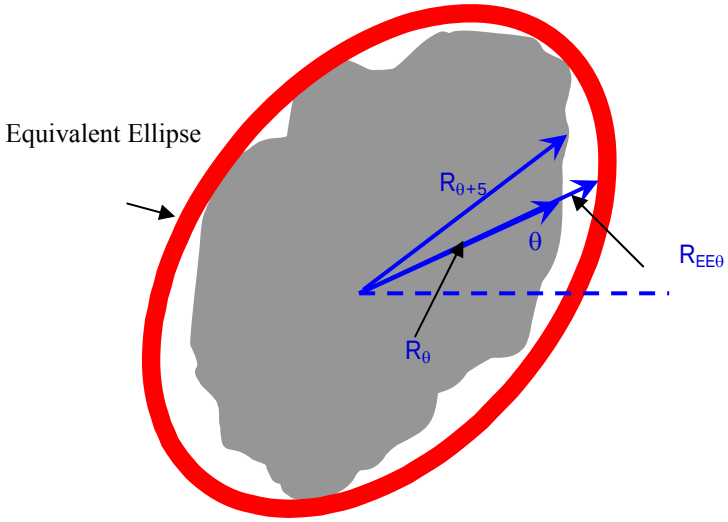

Figure 2. All Illustration of the Radii Used in the Radius Method and Form Index.

The gradient method is based on the concept of gradient vectors. The gradient of an image $f(x,y)$ at location (x,y) is the vector as shown below:

$$\nabla f = \begin{bmatrix} G_x \\ \\ G_y \end{bmatrix} = \begin{bmatrix} \frac{\partial f}{\partial x} \\ \\ \frac{\partial f}{\partial y} \end{bmatrix} \tag{3}$$

It is known from vector analysis that the gradient vector points in the direction of maximum rate of change of f at (x, y). The two important quantities associated with this vector are the magnitude and the direction of this vector. The magnitude of the vector is given by ∇f, where:

$$\nabla f = mag(\nabla f) = \left[G_x^2 + G_y^2\right]^{\frac{1}{2}} \tag{4}$$

The direction of the gradient vector has been used in this project to calculate the measure of angularity of aggregate particles. Let $\theta(x, y)$ represent the direction angle of the vector ∇f at (x, y). Then, vector analysis yields:

$$\theta(x, y) = \tan^{-1}\left(\frac{G_x}{G_y}\right) \tag{5}$$

where the angle is measured with respect to the x axis.

In the gradient method, the direction of the gradient vector for adjacent points changes rapidly at the edge if the corners are sharp. On the other hand, the direction of the gradient vector changes slowly for adjacent points on the edge of the particle for rounded particles. Thus the change in the angle of the gradient vector α for a rounded object is much less compared to the change in the angle of gradient vector for an angular object. Angularity values for all the boundary points are calculated and their sum accumulated around the edge to finally form the angularity index of the aggregate particle. The angularity index is defined as:

$$\text{Angularity Index-Gradient Method} = \sum_{i=1}^{N-3} \left|\theta_i - \theta_{i+3}\right| \tag{6}$$

where the subscript i denotes the i^{th} point on the edge of the particle, and N is the total number of points on the edge of the particle.

Texture analysis is conducted on gray images similar to the one shown in Figure 3. Texture is analyzed with the help of wavelet theory, which presents a multi-scale analysis of textural variation on aggregate images. Wavelet analysis is a powerful method for the

decomposition of the different scales of texture [Mallat 1989]. The wavelet transform works by mapping an image onto a low-resolution image and a series of detailed images. The low-resolution image is obtained by iteratively blurring the original images, eliminating fine details in the image while retaining the coarse details. The remaining detailed images contain the information lost during this operation. The low-resolution image can further be decomposed into the next level of low-resolution and detailed images.

Figure 4 illustrates the Wavelet analysis. The texture information lies in the detail coefficients LH, HL, and HH. The LH coefficients pick up the high-frequency content in the vertical direction, the HL coefficients pick up the high-frequency content in the horizontal direction, and the HH coefficients pick up the high-frequency content in the diagonal direction. Thus, depending upon the selected detail coefficient, directionally oriented texture information can be extracted. Since the directional orientation of the texture content is not emphasized in this project, texture contents in all the directions are given the same weight. Thus, a simple sum of the squares of the detail coefficients (the texture content) is computed as the texture index of the aggregate at that particular resolution. More importantly, detail coefficients have information at different scales, depending upon the level of decomposition. Multi-resolution (or scale) analysis is a very powerful tool that is not possible using a regular Fourier transform.

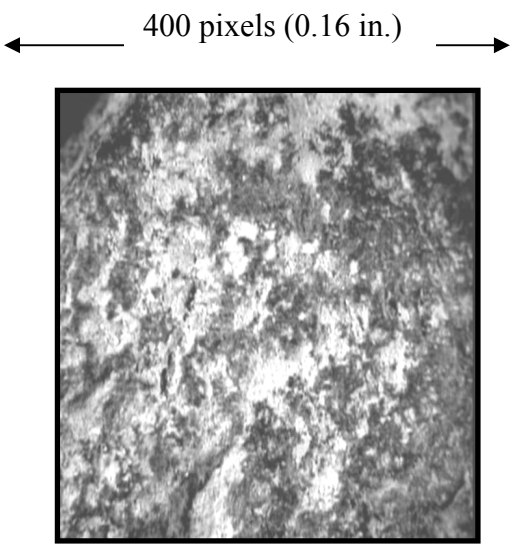

Figure 3. An Example of an Image Used in Texture Analysis.

To describe the texture content at a given resolution or decomposition level, a parameter called the wavelet texture index is defined. The texture index at any given decomposition level is the arithmetic mean of the squared values of the detail coefficients at that level:

$$\text{Texture Index}_n\,(\text{Wavelet Method}) = \frac{1}{3N}\sum_{i=1}^{3}\sum_{j=1}^{N}\left(D_{i,j}(x,y)\right)^2 \qquad (7)$$

where n refers to the decomposition level, N denotes the total number of coefficients in a detailed image of texture; i takes values 1, 2, or 3, for the three detailed images of texture; j is the wavelet coefficient index; and (x, y) is the location of the coefficients in the transformed domain. In this project, the texture is decomposed to six levels. However, only the results from level six are presented since previous research showed that level six was the least affected by color variations and the presence of dust particles on the surface [Fletcher et al. 2003]. The image analysis techniques described above were programmed in a C++ program to facilitate the analysis.

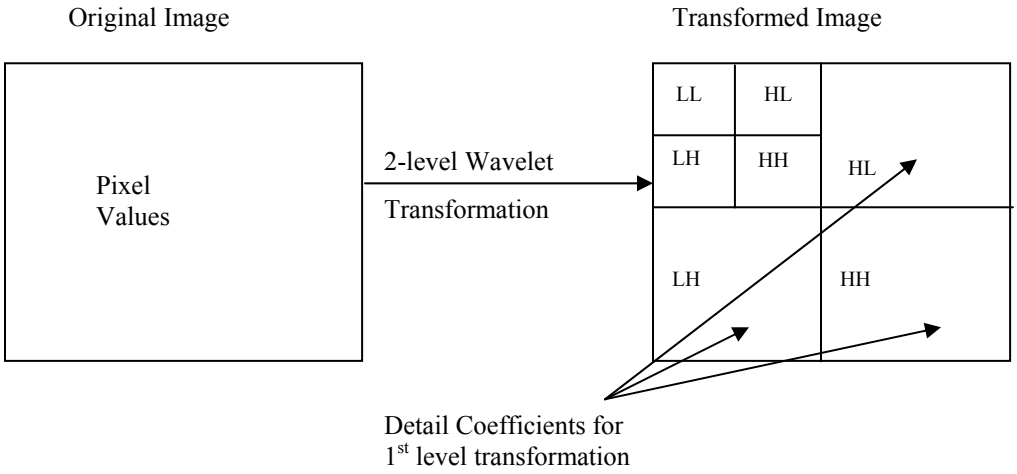

Figure 4. Two-level Wavelet Transformation.

Description of Aggregate Imaging System (AIMS)

Aggregate images were captured using the aggregate imaging system (AIMS) that was developed recently to capture images of both fine and coarse aggregates [Masad 2003]. This system is versatile enough to capture images at different resolutions, field of view, and using different lighting schemes in order to analyze the form, angularity, and texture of fine and coarse aggregates. AIMS utilizes three closed loop DC servo motor linear actuators with 9.84 in. of travel in the *x* and *y*-axes and 1.97 in. of travel in the *z*-axis. This allows for precision movement of all three axes simultaneously and independently from each other. The *x*-axis motion is running

on a slider bar where the camera is attached. The *y*-axis motion of the aggregate tray and back-lit table is running on a bearing guide assembly, which creates smooth uniform motion.

The *z*-axis controls the auto focusing of the camera. The auto focus utilizes high spatial frequency for a signal of a video microscope connected to the camera. The video microscope has a 16:1 zoom ratio, which allows capturing a wide range of particle sizes without changing parts. A black and white video camera with an external control is used. The camera is connected to a magnification lens. The camera and video microscope are attached to a dovetail slide with a motion range of 11.81 in. in the *z*-axis to allow the capture of images of a wide range of aggregate sizes. All motions are connected to a multi-axis external controller that offers both manual and automatic control of motions, as well as enhanced black level and contrast controls. The motion of the microscope, the lighting table, and image acquisition at specified resolutions are all controlled using a program written in Lab View [Masad 2003].

Conventional Tests

Researchers considered the following conventional tests to assess surface properties: fine aggregate angularity (FAA), compacted aggregate resistance (CAR), and flat-elongated test (FE). The experimental procedures followed in the first two tests were based on the Superpave system and according to AASHTO procedures. The method used in the CAR test was based on the current practice as outlined in Shah's master's thesis [Shah 2003]. Brief descriptions of these test methods are given here for completeness.

The National Aggregate Association (NAA) originally developed the FAA test and was later adopted by the ASTM as method C1252 and by AASHTO as method T304. The FAA test measures the loose uncompacted void content of a sample of fine aggregate that fall from a fixed distance through a given sized orifice. A decrease in the void content is associated with more rounded, spherical, smooth surface fine aggregate, or a combination of these factors. Method A of this procedure is used by Superpave to determine aggregate angularity to ensure that fine aggregate has adequate internal friction to provide rut resistance to an HMA.

The CAR test was developed for evaluating shear resistance of compacted fine aggregate in its as-received condition. The test works by applying compressive load on the aggregate specimen using the Marshall testing machine. The compressive load versus displacement is plotted. The maximum compressive load that the specimen can carry is reported as CAR stability value. This value is assumed to be a function of the material shear strength and angularity.

The FE test provides the percentage by number or weight of flat, elongated, or both flat and elongated particles in a given sample of coarse aggregates. The procedure uses a proportional caliper device to measure the dimensional ratio of aggregates. The aggregates are classified according to the undesirable ratios of width to thickness or length to width,

respectively. Superpave specifications characterize an aggregate particle by comparing its length to its thickness or the maximum dimension to the minimum one. In this project, the TxDOT procedure "Tex-280-F" was used to measure the percentage of flat/elongated particles that have the longest dimension to shortest dimension ratio greater or equal to 5.

CHAPTER III
MATERIALS AND MIX DESIGN

Table 1 shows materials selected for this project. One limestone, three siliceous gravels and three granites were selected. The limestone is hard material with low porosity. Gravel-1 is a siliceous river gravel where both fine and coarse fractions were received crushed from the source. Gravel-2 is also siliceous but is comprised of crushed fines and uncrushed coarse aggregate. Gravel-3 is siliceous, and both fine and coarse aggregate portions were uncrushed as received from the source. The image analysis was conducted on material retained on 0.2 in sieve and passing 0.46 in. sieve to represent fine aggregates, and retained on the 0.49 in. sieve and passing the 0.75 in. sieve to represent the coarse aggregates.

Results from Measuring Aggregate Shape Properties

Figures 5, 6, and 7 show the distributions that represent the properties of all aggregates. Statistical parameters such as the median value can be used to represent the entire population as shown in Tables 2 and 3.

Table 1. Aggregate Properties—Conventional Test Results.

Source	Aggregate Type	Aggregate Size and Description	FAA (%) Fine Aggregate Angularity	CAR (lbs) Compacted Aggregate Resistance	Flat & Elongated Particles
Texas	Limestone	Crushed Coarse	--	--	12.50
		Crushed Fine	45.53	4266.70	--
Texas	Gravel-1	Crushed Coarse	--	--	6.40
		Crushed Fine (Crushed Natural Sand)	47.81	5000.00	--
Texas	Gravel-2	Uncrushed Coarse	--	--	3.30
		Crushed Fine (Crushed Natural Sand)	49.85	5000.00	--
Texas	Gravel-3	Uncrushed Coarse	--	--	6.00
		Uncrushed Fine (Natural Sand)	39.00	480.20	--
Oklahoma	Granite-1	Crushed Coarse	--	--	7.90
		Crushed Fine	50.02	4700.00	--
Oklahoma	Granite-2	Crushed Coarse	--	--	15.0
		Crushed Fine	47.39	4450.00	--
Georgia	Granite-3	Crushed Coarse	--	--	5.00
		Crushed Fine	48.00	2232.00	--

Table 2. Median Values of Fine Aggregate Image Analysis Parameters.

Source	Aggregate Type	Radius Angularity	Gradient Angularity	Form_2D	Texture
Texas	Limestone	11.19	2652.38	6.59	192
Texas	Gravel-1	12.80	2611.39	9.40	96.00
Texas	Gravel-2	14.83	3532.02	7.78	100.00
Texas	Gravel-3	9.27	2044.5	5.95	93.00
Oklahoma	Granite-1	17.04	5128.38	8.44	197.00
Oklahoma	Granite-2	19.07	3157.37	9.73	126.80
Georgia	Granite-3	17.99	4401.4	7.87	145.00

Table 3. Median Values of Coarse Aggregate Image Analysis Parameters.

Source	Aggregate Type	Radius Angularity	Gradient Angularity	Form_2D	Texture
Texas	Limestone	15.50	3041.00	7.15	245.50
Texas	Gravel-1	11.71	2926.85	6.30	110.00
Texas	Gravel-2	9.90	1725.24	5.77	91.00
Texas	Gravel-3	10.09	1936.26	5.39	150.00
Oklahoma	Granite-1	13.96	2988.81	8.29	276.00
Oklahoma	Granite-2	14.59	2728.66	9.10	150.00
Georgia	Granite-3	12.77	3347.32	6.52	422.00

Figure 5 shows that among all the fine aggregates tested, the granites are most angular while the uncrushed river gravel is least angular as measured by both the radius and gradient methods. We observed that form values were also higher for the granites compared with other aggregates. Both limestone and granites possess higher texture values compared to gravels as shown in Figure 7 (a).

Coarse aggregate image analysis results show that limestone is most angular when evaluated via the radius method while Granite-3 is most angular when the evaluation is via the gradient method (Figure 6). This result is because the gradient method captures very small surface irregularities while measuring angularity of a particle [Fletcher et al. 2003]. In the case of coarse aggregate texture as shown in Figure 7 (b), both the limestone and the granites show a higher level of texture as compared to the gravels. The texture of the coarse fraction of the Granite-3 aggregate is the highest.

Figures 5 and 6 illustrate that radius angularity has a tighter distribution (less spread) than gradient angularity and that gradient angularity provides a superior means by which to differentiate among aggregates. All seven aggregates were analyzed using the Tukey's statistical test for multiple comparisons. This analysis was performed separately for fine and coarse material. The analysis results showed that gradient angularity values overlap less and have a larger spread than radius angularity as shown in Table 4. This trend was found for both fine and coarse aggregates. The statistical analysis results confirm that the gradient method can differentiate between aggregates better than the radius method.

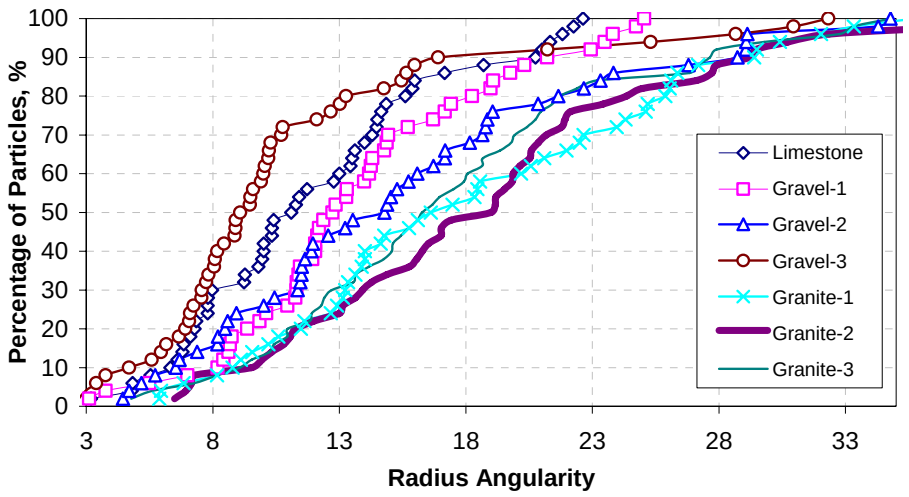

(a)

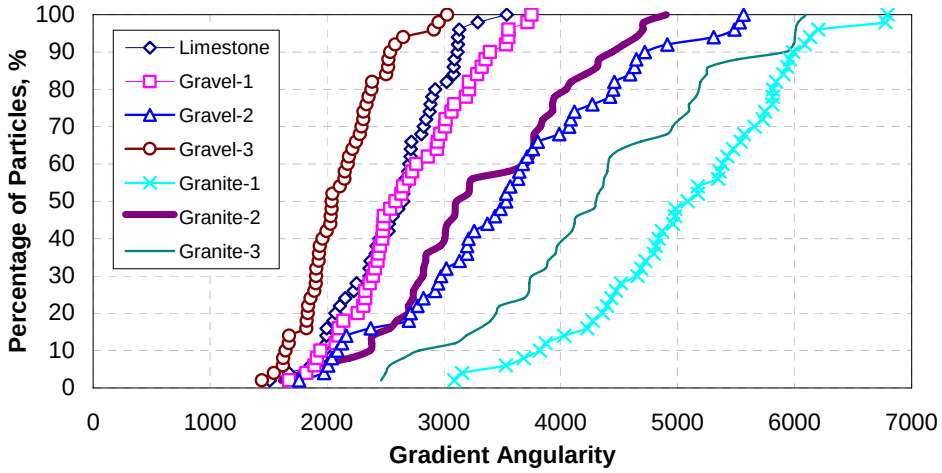

(b)

Figure 5. Angularity Values of All Fine Aggregates (a) Radius Angularity (b) Gradient Angularity.

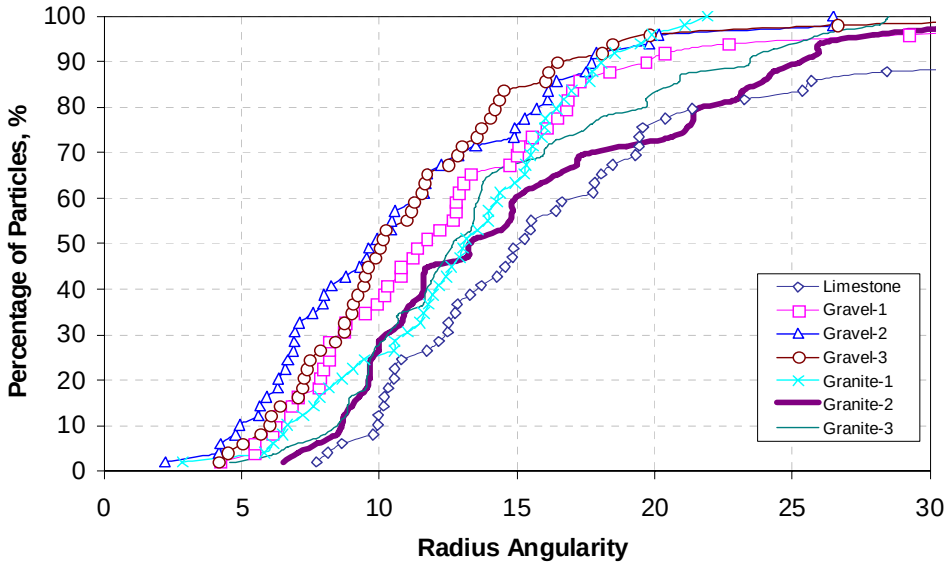

(a)

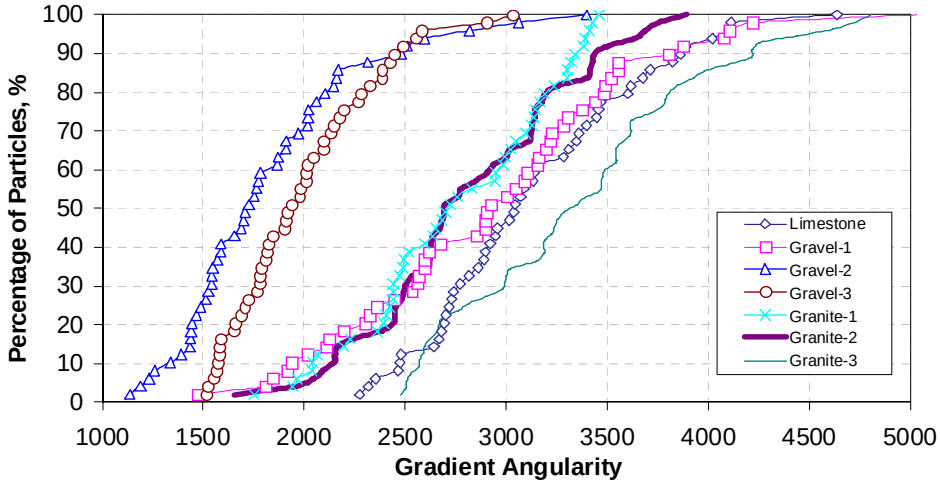

(b)

Figure 6. Angularity of All Coarse Aggregates

(a) Radius Angularity (b) Gradient Angularity.

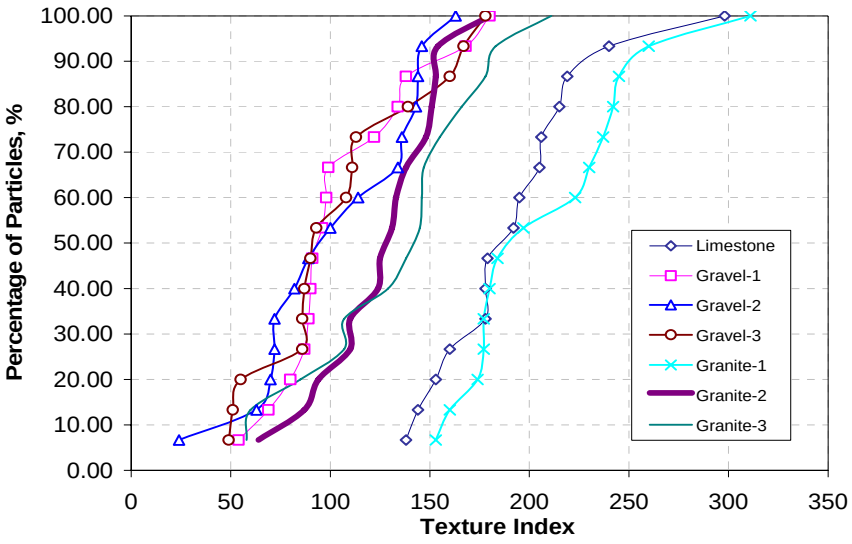

(a)

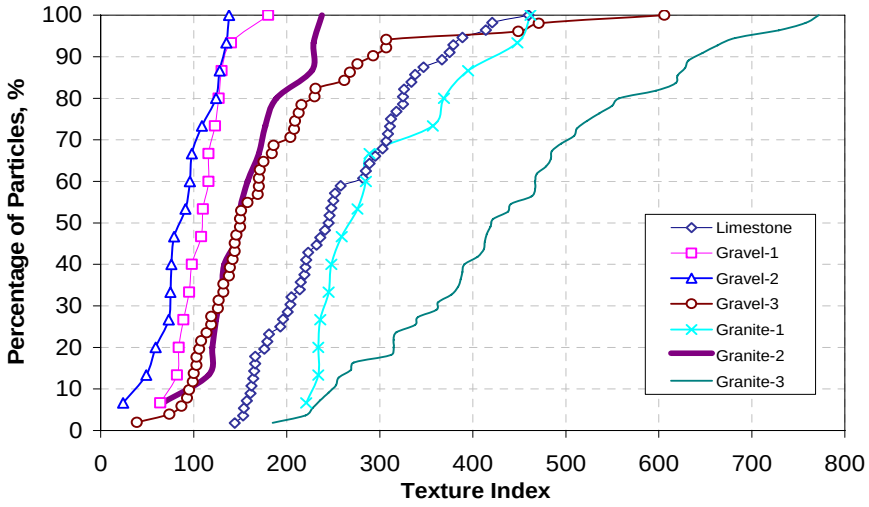

(b)

Figure 7. Texture Index of All Aggregates

(a) Fine Aggregates (b) Coarse Aggregates.

Table 4. Statistical Analysis: Tukey's Test Results of Coarse Aggregates.

(a) Coarse Aggregate-Radius Angularity

Aggregate Type	No. Particles	Subset for alpha = .05		
		1	2	3
Gravel-2	50	A		
Gravel-3	50	A	B	
Gravel-1	50	A	B	
Granite-3	50	A	B	C
Granite-1	50	A	B	C
Granite-2	50		B	C
Limestone	50			C

(b) Coarse Aggregate-Gradient Angularity

Aggregate Type	No. Particles	Subset for alpha = .05				
		1	2	3	4	5
Gravel-2	50	A				
Gravel-3	50		B			
Granite-2	50			C		
Gravel-1	50				D	
Granite-1	50				D	
Limestone	50				D	
Granite-3	50					E

Image analysis testing was performed on limestone, Gravel 3, Granite-1, and Granite-3. after crushing in the laboratory using a cone crusher. The effect of crushing on the individual aggregates is summarized as follows:

- Neither Granite-1 nor Granite-3 showed a significant change in parameters derived from image analysis (e.g., form, angularity, or texture) due to the effects of crushing. This result is not surprising and even reinforces the efficacy of image analysis as the granites were crushed at the production plant prior to original image analysis testing.
- The texture did not change significantly after crushing for either the limestone or Gravel-3.

Figure 8 shows that the gradient value for Gravel-3 increased after crushing but the texture value didn't change significantly (Figure 9). These results are in agreement with previous findings that crushing of siliceous gravels improves angularity, but has little effect, if any, on texture [Fletcher et al. 2003].

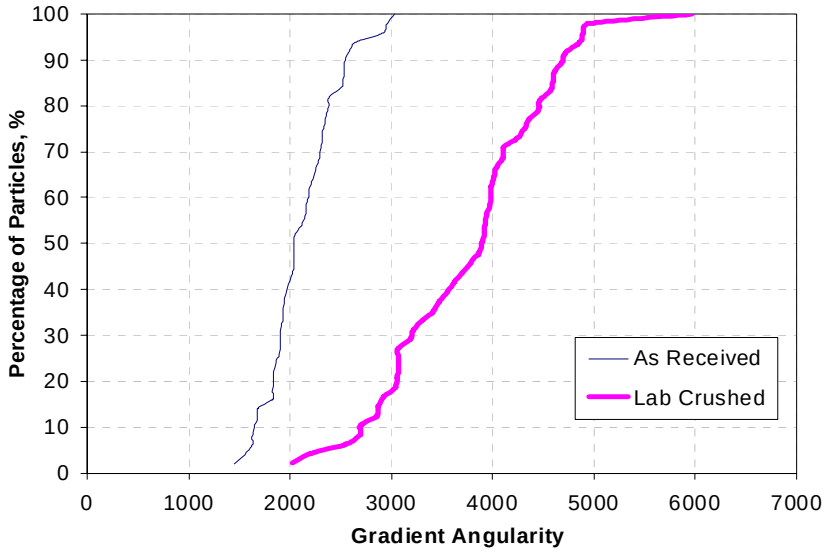

Figure 8. Effect of Crushing on Gradient Angularity of Gravel-3 Aggregate.

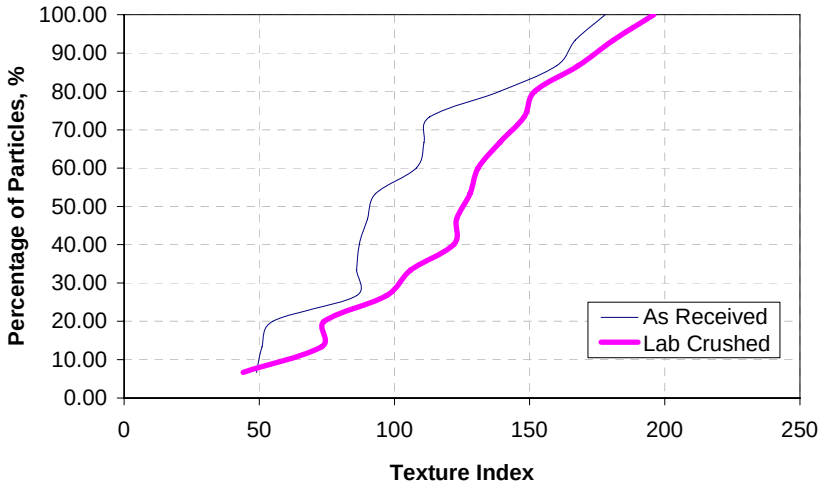

Figure 9. Effect of Crushing on Texture Index of Gravel-3 Aggregate.

Table 1 shows aggregate properties as measured by conventional methods. Both the fine aggregate angularity method and the compacted aggregate resistance method show that Gravel-3 is least angular. Furthermore, these two methods show that crushed gravels, Gravel-1, and Gravel-2, are more angular compared to limestone. Granite-2 was found to have the highest flat and elongated values. Image analysis results were compared to conventional test results like fine aggregate angularity, compacted aggregate resistance, and flat and elongated results. A reasonable correlation was observed between flat and elongated test results and form index value of coarse aggregates ($R^2 = 0.58$). A correlation with $R^2 = 0.5$ was observed between the uncompacted void content (FAA) values versus radius and gradient angularity values of fine aggregates. No correlation was observed between the compacted aggregate resistance values versus radius and gradient angularity values of fine aggregates.

Sensitivity of HMA Performance to Aggregate Shape

Four of the aggregates were used to prepare asphalt mixes using the Superpave mix design procedure for a traffic level between 10 to 30 million equivalent single axle load's (ESAL). Gradations were kept almost the same for all mixes. Specimens for the volumetric analysis were compacted using the Superpave gyratory compactor to 109 gyrations (N_{des}). The binder selected for this project was PG 64-22. The mixing and compaction temperature for the binder selected, as measured by the Superpave method, was 320 °F (160 °C) and 295 °F (146 °C), respectively. Table 5 shows the mix design information.

Table 5. Mixture Design Information.

Mixture Type	Binder Content (%)	Binder Type	Maximum Specific Gravity	Void in Mineral Aggregate %	Aggregate Bulk Specific Gravity
Limestone	4.85	PG 64-22	2.478	14.72	2.65
Gravel-1, crushed	5.60	PG 64-22	2.421	16.29	2.62
Granite-3, crushed	4.46	PG 64-22	2.471	15.14	2.69
Gravel-3, uncrushed	3.60	PG 64-22	2.484	11.44	2.60

The aggregates selected for the performance tests were: Limestone, Gravel-1, Gravel-3, and Granite-3. The aggregates represent considerable variations in surface properties. Table 1 summarizes conventional test results on these aggregates. These results show that fine Gravel-1 is more angular compared to the limestone based on both the uncompacted void content method and the compacted aggregate resistance methods. The image analysis results show that the angularity of fine Gravel-1 is comparable to that of limestone. However, the texture of fine limestone, and angularity and texture of coarse limestone are higher than Gravel-1. In general, the image analysis results favor the limestone over Gravel-1. On the basis of image analysis

results, these four mixtures should exhibit resistance to rutting from best to worse in the following order: Granite-3, Limestone, Gravel-1, and Gravel-3.

Performance related tests were conducted to rank the susceptibility of mixtures prepared with the selected aggregates to permanent deformation. The tests selected were the asphalt pavement analyzer (APA), Hamburg wheel tracking device (HW), and dynamic modulus test (DM).

The APA test was performed under dry conditions following the protocol documented by Pavement Technology, Inc. [APA 1998]. The rut-depth evaluation is typically determined after 8000 load cycles are applied to 6-inch by 3-inch cylindrical samples compacted to 7 percent air void. The wheel load is usually 100 lb (445 N), and the hose pressure is 100 psi (690 kPa). Higher wheel loads and contact pressures can also be used. APA testing can be performed using chamber temperatures ranging from 41 °F to 160 °F (5 °C to 71 °C). A temperature of 130 °F (54.4 °C) was selected for this project. Figure 10 shows results of two replicates tested.

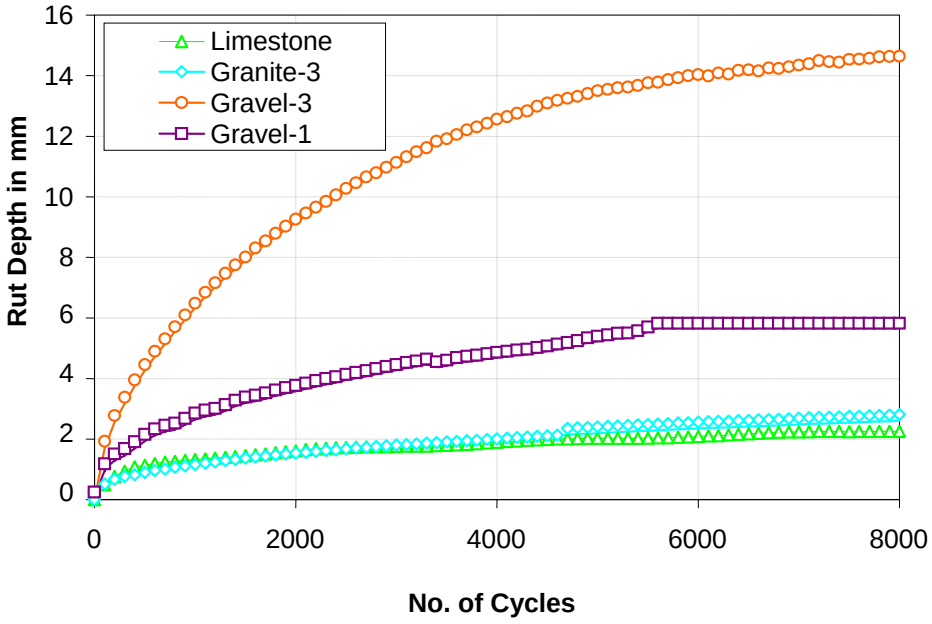

Figure 10. APA Test Results of Mixes with Different Aggregates (1 in. = 25.4 mm).

The HW test was performed following the protocol in TxDOT test method "Tex-242-F." This is similar to the one described by Aschenbrener (1996). The test was conducted under

water at a constant temperature of 122 °F (50°C). In the Hamburg test, the sample is loaded with a reciprocating motion of the 1.85 in. wide steel wheel using a 158-lb force (705 N).

The test was conducted to 20,000 cycles or to a specified rut depth or 0.49 in. Rut depth is measured at several locations, including the center of the wheel travel path, where it usually reaches the maximum value. The samples were compacted to 7 percent air voids. Superpave gyratory samples with a diameter of 6 inches and a thickness of 2.5 inches (15 cm diameter and about 6.35 cm high) were tested, and the results are shown in Figure 11.

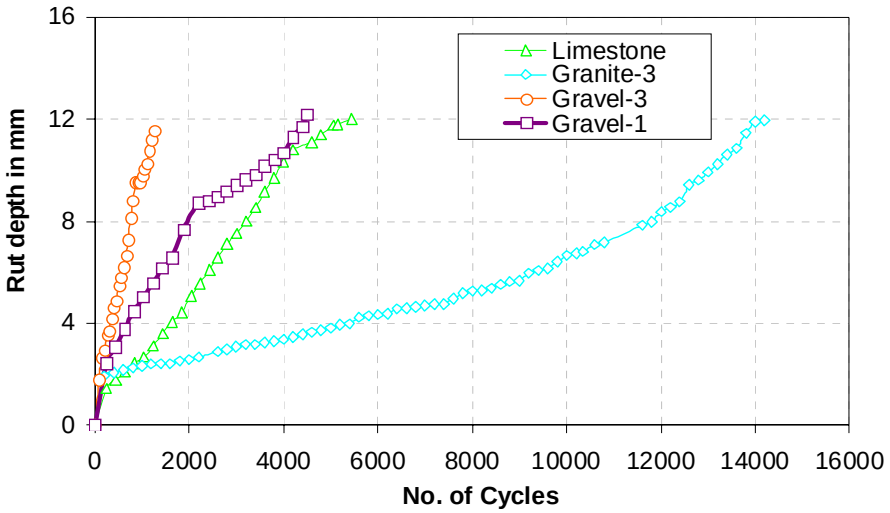

Figure 11. Hamburg Test Results of Mixes with Different Aggregates (1 in. = 25.4 mm).

Mixes were also tested using a compressive dynamic test to measure the dynamic modulus as a function of number of cycles. The test was conducted according to the procedure outlined in Shah's master's thesis [Shah 2003]. Samples for each type of mix were subjected to cyclic testing in both dry and wet testing conditions. Samples were preconditioned before testing. Dry samples were kept in an oven at 104 ^{o}F (40 °C), and wet samples were soaked in water at 104 ^{o}F (40 °C) until they reached at least 85 percent saturation. After preconditioning, the samples were loaded in materials testing system (MTS) machine. This machine is used to apply a repeated unconfined compressive load to the sample in a controlled stress mode. The test is performed at a loading frequency of 1 Hz of haversine wave loading for 20,000 cycles. The permanent deformation of a sample is determined by measuring the micro strain obtained through two linear variable differential transducers (LVDTs) on the periphery of the sample. The samples were compacted to 4 percent air voids and two replicate samples (4 inches in diameter and 6 inches high) were tested. The dynamic modulus is obtained by dividing the applied stress by the resilient strain at the end of each cycle, and the results are as shown in

Figure 12. The average rutting in the APA was 0.57 in. in the case of the Gravel-3 mixtures after 8000 cycles while there was no significant rutting in the case of limestone and Granite-3 mixtures. Approximately 0.09 in. of rutting was observed in the case of limestone while 0.11 in. of rutting was observed in the case of Granite-3 after 8000 cycles. In the case of the Gravel-1 mixture, an average rutting of 0.26 in. was observed after 8000 cycles (Figure 10).

Figure 11 shows Hamburg test results. Granite-3 reached a maximum rut depth of 0.49 in. in an average of 14,200 cycles; limestone reached the 0.49 in. rut depth mark in 5451 cycles; Gravel-1 reached the 0.49 in. rut depth mark in 4500 cycles; and Gravel-3 reached the 0.49 in. rut depth mark in 1280 cycles. The results suggest that performance of the granite mix is superior to the limestone mix under wet conditions, as evaluated in the HW test. This might indicate that the granite, which has higher texture and angularity, retained a superior level of bonding in the presence of water compared with the limestone aggregate. In order to fully assess the bonding between the binder and aggregate, it is also necessary to calculate the chemical bonding energy or adhesive bond between the asphalt and aggregate in the presence of water. Such calculations have been made and are discussed by Cheng et al. [Cheng et al. 2002].

The performance of crushed gravel in wet tests was better as compared to uncrushed gravel, whereas in the case of dry tests there was no improvement observed in the performance of crushed gravel. Limestone performed better in both wet and dry tests as compared to crushed gravel. Also, these results show that granite performed better in the wet condition compared to limestone. However, in the dry condition both aggregates demonstrated comparable (almost identical) performance. In the dry condition as shown in Figure 12 (a), the dynamic modulus of mixtures with both granite and limestone aggregates was approximately 18,000 psi. In wet conditions as in Figure 12 (b), dynamic modulus of granite was around 12,500 psi; whereas that of limestone was only about 5500 psi. In addition, mixtures prepared with granite aggregate showed the highest wet/dry ratios of dynamic modulus compared to the other three aggregate mixtures. This supports the findings from APA and HW that granite, due to its high texture, might retain more bonding with the binder and exhibit higher resistance to deformation under wet conditions compared with limestone. Of course, the chemical surface properties of the granite must have contributed to this performance and must be considered in a complete analysis.

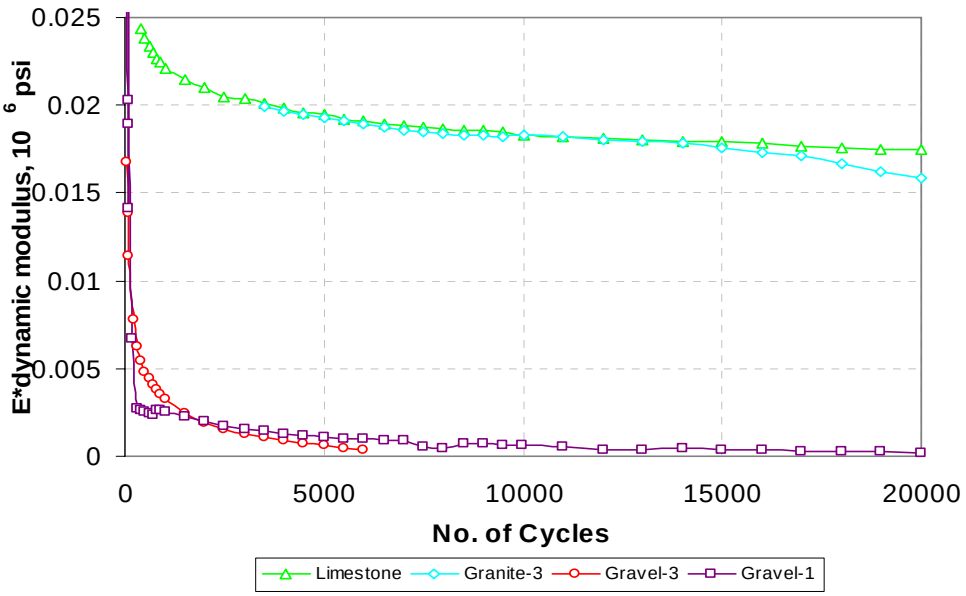

(a)

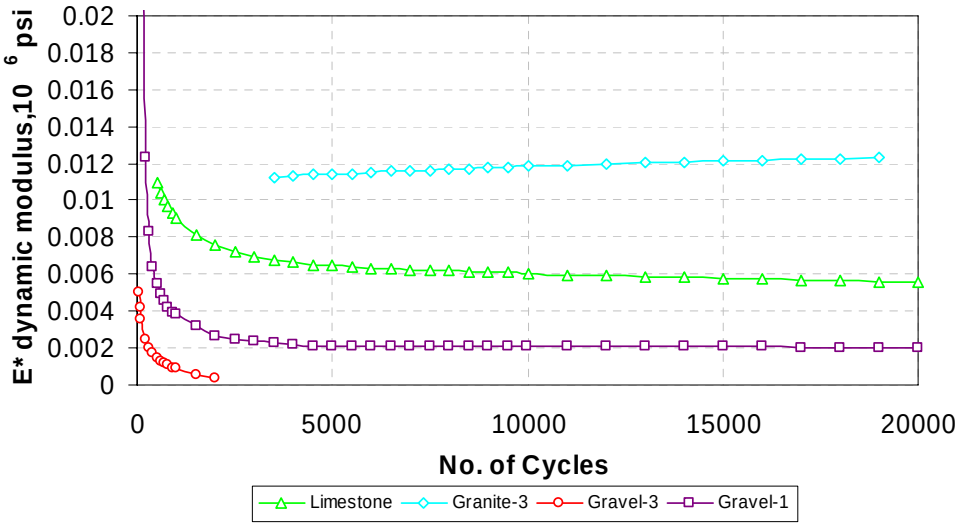

(b)

Figure 12. Modulus (E*) Values of Mixes with Different Aggregates (a) Dry Conditions (b) Wet Conditions.

CHAPTER IV
CONCLUSIONS

Based on the findings of test results and data analysis, the following conclusions may be drawn:

- Aggregate angularity is a critically important physical aggregate property. Gradient angularity is superior to radius angularity in its ability to characterize aggregate angularity and as a tool by which to assess the effects of angularity on mixture performance. This assessment is based on two factors: (1) the range of gradient angularity values is substantially greater for the diverse aggregates evaluated than the range in radius angularity values. (2) The gradient angularity value predicted performance better than conventional test values.
- Image property tests performed on aggregates before and after crushing demonstrated that image analysis parameters are sensitive to the effects of crushing on surface shape. Crushing changed the angularity of the siliceous river gravel but did not influence texture. In the case of the granite aggregates, laboratory crushing did not affect angularity and form properties as defined by image analysis in two of the three granites. This is not surprising based on the fact that the granites were previously crushed during production.
- While a reasonable correlation was found between fine aggregate angularity and angularity based on image analysis, no correlation was observed between compacted angularity and angularity based on image analysis. However, image analysis values were able to rank the performance tests in order of rutting susceptibility, especially under wet testing conditions. As a specific example, Gravel-3, crushed gravel, was predicted to perform better than limestone based on conventional test results. However, image analysis (gradient angularity, texture) predicted the opposite in terms of performance, and this was actually the case.
- The dynamic modulus test results were similar for mixtures prepared with limestone and granite aggregates in the dry condition. This was also the case in APA testing. However, the relative impact of moisture conditioning on mixtures prepared with granite, as indicted using the dynamic modulus and Hamburg tests, was less than on mixtures prepared from limestone aggregates. This was consistent with image testing (gradient angularity and texture), which predicted that the granite aggregate has higher texture and, consequently, would have better adhesive bonding with asphalt than the limestone aggregate.

CHAPTER V

REFERENCES

Aschenbrener, T., "Evaluation of Hamburg Wheel-Tracking Device to Predict Moisture Damage in Hot-Mix Asphalt," *Transportation Research Record 1492*, Transportation Research Board, National Research Council, Washington, D.C. 1996, pp. 193-201.

Cheng, D., Little, D. N., Lytton, R. L., and Holste, J., "Use of Surface Free Energy Properties of the Asphalt-Aggregate System to Predict Damage Potential," *Journal of the Asphalt Paving Technologists*, Vol. 71, 2002, pp. 59-88.

Fletcher, T., Chandan, C., Masad, E., and Sivakumar, K., "Aggregate Imaging System (AIMS) for Characterizing the Shape of Fine and Coarse Aggregates," *Transportation Research Record 1832, Journal of the Transportation Research Board*, 2003, pp. 67-77.

Huber, G. A., Jones, J. C., and Jackson, N. M. "Contribution of Fine Aggregate Angularity and Particle Shape to Superpave Mixture Performance," In *Transportation Research Record 1609, Journal of the Transportation Research Board*, 1998, pp. 28-35.

Mallat, S. G., "A Theory for Multiresolution Signal Decomposition: The Wavelet Representation," *IEEE Transactions on Pattern Analysis and Machine Intelligence*, Vol. II, 1989, No. 7.

Masad, E., "The Development of a Computer Controlled Image Analysis System for Measuring Aggregate Shape Properties," NCHRP-IDEA Project 77 Final Report, Transportation Research Board, 2003, Washington, DC.

Masad, E., Olcott, D., White, T., and Tashman, L., "Correlation of Fine Aggregate Imaging Shape Indices with Asphalt Mixture Performance," *Transportation Research Record 1757,* Transportation Research Board, National Research Council, Washington D.C., 2001, pp. 148-156.

McGennis, R. B., Andersen, R. M., Kennedy, T. W., and Solaimanina, M., "Background of SUPERPAVE Asphalt Mixture Design and Analysis," Final Report No. FHWA-SA-95-003, Federal Highway Administration, U.S. Department of Transportation, Washington, D.C., 1995.

Pavement Technology, *Asphalt Pavement Analyzer User's Guide*. Pavement Technology, Inc., Covington, Georgia, 1998.

Shah, B., "Evaluation of Moisture Damage within Asphalt Concrete Mixes," Master's Thesis, Texas A&M University, College Station, Texas, 2003.